ORIGINAL RESEARCH ARTICLE

Identification of murine Phosphodiesterase 5A isoforms and their functional characterization in HL-1 cardiac cell line†

Federica Campolo[1], Alessandra Zevini[2], Silvia Cardarelli[3], Lucia Monaco[4], Federica Barbagallo[1], Manuela Pellegrini[5], Marisa Cornacchione[2], Antonio Di Grazia[2], Valeria De Arcangelis[2], Daniele Gianfrilli[1], Mauro Giorgi[3], Andrea Lenzi[1], Andrea M. Isidori[1], Fabio Naro[2*]

[1]*Department of Experimental Medicine, Sapienza University, Rome, Italy;*
[2]*Department of Anatomical, Histological, Forensic Medicine and Orthopedic Sciences, Sapienza University, Rome, Italy;*
[3]*Department of Biology and Biotechnology "Charles Darwin", Sapienza University, Rome, Italy;*
[4]*Department of Physiology and Pharmacology, Sapienza University, Rome, Italy;*
[5]*Institute of Cell Biology and Neurobiology, CNR, Monterotondo, Rome, Italy.*

***Corresponding author:**
Fabio Naro, Prof, MD
DAHFMO, Sapienza University
Via Scarpa, 16, 00131 Rome, Italy
Phone:+39- 06-49766587; Fax:+39-06-4462854
E-mail: fabio.naro@uniroma1.it

Running title: PDE5A isoforms in cardiac hypertrophy

Fundings: Contract grant sponsor: MIUR; contract grant number: FIRB 2010 RBAP109BLT, RBFR10URHP, FIRB 2012 RBFR12FI27 to AL, FN and FB respectively and PRIN 2010 KL2Y73-006 to FN. Contract grant sponsor: AFM; contract grant number: 15586 to LM.

†This article has been accepted for publication and undergone full peer review but has not been through the copyediting, typesetting, pagination and proofreading process, which may lead to differences between this version and the Version of Record. Please cite this article as doi: [10.1002/jcp.25880]

Additional Supporting Information may be found in the online version of this article.

Received 21 October 2016; Revised 27 January 2017; Accepted 27 February 2017
Journal of Cellular Physiology

DOI 10.1002/jcp.25880

ABSTRACT

Phosphodiesterase 5A (PDE5A) specifically degrades the ubiquitous second messenger cGMP and experimental and clinical data highlight its important role in cardiac diseases. To address PDE5A role in cardiac physiology, three splice variants of the PDE5A were cloned for the first time from mouse cDNA library (mPde5a1, mPde5a2 and mPde5a3). The predicted amino acidic sequences of the three murine isoforms are different in the N-terminal regulatory domain. mPDE5A isoforms were transfected in HEK293T cells and they showed high affinity for cGMP and similar sensitivity to sildenafil inhibition. RT-PCR analysis showed that *mPde5a1, mPde5a2* and m*Pde5a3* had differential tissue distribution. In the adult heart, m*Pde5a1* and m*Pde5a2* were expressed at different levels whereas m*Pde5a3* was undetectable. Overexpression of mPDE5As induced an increase of HL-1 number cells which progress into cell cycle. mPDE5A1 and mPDE5A3 overexpression increased the number of polyploid and binucleated cells, mPDE5A3 widened HL-1 areas and modulated hypertrophic markers more efficiently respect to the other mPDE5A isoforms. Moreover, mPDE5A isoforms had differential subcellular localization: mPDE5A1 was mainly localized in the cytoplasm, mPDE5A2 and mPDE5A3 were also nuclear localized. These results demonstrate for the first time the existence of three PDE5A isoforms in mouse and highlight their potential role in the induction of hypertrophy.

Keywords: PDE5A isoforms; cardiomyocytes; hypertrophy; polyploidy

INTRODUCTION

Phosphodiesterases (PDEs) are a large family of enzymes which hydrolyze the second messengers cAMP and/or cGMP playing a critical role in the regulation of cell response to different stimuli. Each member of PDE family consists of multiple variants produced by alternative splicing and/or usage of different transcription initiation sites (Conti and Beavo, 2007). PDE isoforms might show different hydrolytic kinetic and substrate affinity in specific tissues and a different cellular distribution (Lin et al., 2006). Among the other PDEs a great interest is given to PDE5A, a cGMP hydrolyzing enzyme, since its inhibition results useful for the treatment of erectile dysfunction (Goldstein et al., 1998) and, possibly, for cancer (Catalano et al., 2016; Zhu et al., 2005) and heart diseases (Lukowski et al., 2014).

Regarding the expression in the tissues, in rodents *Pde5a* mRNA was found in platelets, lung, and cerebellum, brain, kidney, liver and heart (Kotera et al., 2000), in felines it was found in the heart (Shan and Margulies, 2011), and in dogs it was present at high levels in the lung (Lin et al., 2006). In human the highest levels of *Pde5a* mRNA were found in the cerebellum, kidney, pancreas, lung and heart (Kotera et al., 2000). PDE5A protein was detected at high levels in human platelets, lung, smooth muscle, including the vascular tissues of penis, brain and cerebellum, where it is particularly abundant in Purkinje neurons (Giordano et al., 2001; Shimizu-Albergine et al., 2003).

In the heart, PDE5A regulates vascular tone, cardiomyocyte contraction, mitochondrial function and stress-response signaling (Isidori et al., 2015; Tsai and Kass, 2009). In adult cardiomyocytes PDE5A localizes at the z-disks of sarcomere and under the sarcolemma where it can degrade a cGMP pool generated by soluble guanylyl cyclase (sGC) (Takimoto et al., 2005). Upregulation of PDE5A expression was reported occurring in several cardiac pathological conditions (Pokreisz et al., 2009) and its inhibition leads to prevention and reversion of cardiac hypertrophy (Takimoto et al., 2005).

Like for other PDEs, several isoforms exist for PDE5A. Three isoforms were identified in humans (PDE5A1, PDE5A2 and PDE5A3) (Kotera et al., 1998; Lin et al., 2000b). These proteins differ in the 5' terminus of the respective mRNAs and consequently in the corresponding amino acid sequence at the N-terminus. The human PDE5A gene contains 21 exons spanning approximately 100 kb and encodes three different mRNAs (Yanaka et al., 1998). These transcripts are yielded by the splicing of three alternative first exons in the pre-mRNA. PDE5A1 lengths for 875 amino acids, PDE5A2 for 833 amino acids and PDE5A3 for 823 amino acids. All three isoforms had similar cGMP-catalytic activities and similar inhibition sensitivity to sildenafil and zaprinast (Lin et al., 2000a). Whereas PDE5A1 and PDE5A2 isoforms are expressed in all human tissues, PDE5A3 is

restricted to smooth muscle and cardiac muscle tissues. In mouse was identified so far only one isoform localized in chromosome 3 and corresponding to *Pde5a1* (NM_153422.2) (Burns et al., 1996).

In order to address the physiological role of PDE5A in mouse cardiac muscle, the existence of additional isoforms was investigated. Three new isoforms were identified, cloned, biochemically characterized and their tissue expression evaluated. Flow cytometry and morphological analyses revealed specific biological activity of each isoform in cardiac cell line.

MATHERIAL AND METHODS

Ethics statement

All procedures involving mice were approved by the Italian Ministry of Health and permission by the Animal Care and Committee of Sapienza University was received. The procedures were performed according to the ethical guidelines for animal care of the European Community Council (directive 86/609/ECC).

Mice

CD1 mice of 60 dpp were obtained from Charles River Laboratories Italia (Calco, Lecco, Italy) and used in this study. At least 3 adult male and female (2-4 months of age) were used for organs collection in different experiments. For cardiomyocyte preparation were used 13-15 embryos (13.5 dpc) or neonatal (1 dpp) mice. For adult cardiomyocyte preparations were used 3 mice. All mice were sacrificed by cervical dislocation.

Plasmids

Murine PDE5A isoforms were cloned into pCDNA3.1 and pEGFPC1 expression vectors respectively. PDE5A1 was cloned in the pCDNA3.1 expression vector between the EcoRV (5') and XbaI (3') restriction sites. PDE5A2 and PDE5A3 isoforms were cloned into pCDNA3.1 through replacement of the N-terminus of PDE5A1. The N-terminus of PDE5A2 (NCBI accession number KR816338.1) and PDE5A3 were amplified from whole murine embryonic RNA by RT-PCR using a reverse primer that annealed to a sequence including the KpnI site at 1600 bp of PDE5A sequence, and a forward primer that introduced a KpnI restriction site at the 5' end of the product. Murine PDE5A isoforms were also cloned in pEGFP-c1 vector between the XhoI (5') and SalI (3') restriction sites. All generated plasmids were sequenced.

Cell cultures and transfection

Primary cultures of mouse cardiomyocytes were prepared from 13.5 dpc hearts according to (Isidori et al., 2015) and from 1 dpp hearts as following: hearts were rapidly excised and placed into Hank's solution, atria were cut off and ventricles were minced and digested by sequential incubation at 37°C for 15 min with 100 μg/ml collagenase type II (Gibco-Life Technology, CA, USA) and 900 μg/ml pancreatin (Sigma Aldrich, CA, USA) in ADS buffer (0.5M NaCl, 0.1M KCl, 0.1M glucose, 0.1M hepes, 0.1M NaH_2PO4, 0.1M $MgSO_4$). Cells were resuspended in Dulbecco's modified Eagle's medium containing 10% v/v horse serum (Gibco-Life technology, CA, USA), 5% v/v fetal bovine serum (FBS) and 10 mg/ml gentamicin (Sigma Aldrich, CA, USA) and plated for 2 hours at 37°C to remove the contaminating fibroblasts. The unattached cells were collected and plated onto collagen-coated tissue culture dishes in Dulbecco's modified Eagle's medium containing 10% v/v horse serum, 5% v/v FBS and 10 mg/ml gentamicin at a density of 3×10^5 cardiac cells per 35-mm Petri dishes.

HL-1 cells, kindly provided by Dr. Simona Nanni (Catholic University, Rome, Italy), were cultured in Claycomb medium (Sigma Aldrich, CA, USA) supplemented with 10 % v/v FBS (Sigma Aldrich, CA, USA), 0.2 mM norepinephrine, 2 mM L-glutamine, 1 U/ml penicillin and 1 μg/ml streptomycin solution (Sigma Aldrich, CA, USA) as previously described (Claycomb et al., 1998).

NIH3T3 and HEK293T cell lines (ATCC, VA, USA) were maintained in Dulbecco's modified Eagle's medium supplemented with 10% v/v FBS, non-essential amino acids solution (Life Technologies, CA, USA) 2 mM L-glutamine, 1 U/ml penicillin and 1 μg/ml streptomycin solution (Sigma Aldrich, CA, USA). HL-1 transfection was performed using Lipofectamine 3000 (Life Technologies, CA, USA). Briefly 5 x 10^5 HL-1/well were plated in 3.5 cm dishes and transfected after 24 h with PDE5A isoforms GFP-tagged vectors. Several DNA concentrations were tested and the lowest DNA concentration useful to achieve mPDE5A isoforms overexpression was used. Isoforms transfection efficiency ranged between 18-25% after 24h (Fig. S2C).

Phosphodiesterase activity assay

Cells were homogenized using a glass homogenizer (15 strokes, 4°C) in 20 mM Tris-HCl buffer pH 7.2 containing 0.2 mM EGTA, 5 mM β-mercaptoethanol, 2% v/v antiprotease cocktail (Sigma Aldrich, CA, USA), 1 mM PMSF, 5 mM $MgCl_2$, 0.1% v/v Triton X-100. The homogenates were centrifuged at 14000 g for 30 min at 4°C and pellets were re-suspended in the homogenization buffer and centrifuged at 14000 g for 30 min at 4°C. The first and second supernatants were then pooled and used for further analyses. PDE activity was measured at 30°C with the two-step method

described by Thompson and Appelman (Thompson and Appleman, 1971), using [H^3]cGMP (Perkin Elmer, MA, USA). Aliquots of extracts were incubated in 60 mM HEPES pH 7.2 assay buffer containing 0.1 mM EGTA, 5 mM $MgCl_2$, 0.5 mg/ml bovine serum albumin, 30 µg/ml soybean trypsin inhibitor, in a final volume of 0.3 ml. The reaction was started by adding tritiated substrate at indicated concentrations and stopped by adding 0.1 M HCl. For IC_{50} experiments, indicated sildenafil concentrations were added to the reaction mix. To evaluate the enzymatic specific activity (µmoles cGMP hydrolyzed/min./mg of enzyme), protein extracts from HEK293T, transfected with the indicated PDE5A isoforms, were assayed for PDE activity and 30 pmoles of cGMP hydrolytic activity for each sample were loaded onto a polyacrylamide gel, electrotransferred on PVDF membrane and probed with rabbit polyclonal PDE5A antibody. The amount of PDE5A in each immunoreactive band was evaluated by densitometric analysis and compared to different concentrations of purified mouse recombinant PDE5A (Abcam, UK).

RT-PCR and RT-qPCR

Total RNA was isolated from tissue samples or cell lines using TRIzol® reagent (Life Technologies, CA, USA) according to manufacturer's instruction. 1 µg of RNA was DNAse treated (Zymo Research, CA, USA) and reverse transcribed with random hexamer primers using a cDNA synthesis Kit (Promega, Mannheim, Germany). Primer sets used for semi-quantitative RT-PCR are: PDE5A1 Fw 5'-CACCATGGAACGAGCGGGCCCCAACTC-3', PDE5A2 Fw 5'-ATGTTGCCCTTTGGAGACAAAACG-3', PDE5A3 Fw 5'-GTTTTGTTCTACAGAGACATG-3', PDE5A1-2-3 Rev 5'-CTTGAGCACTGGTCCCCTTCATC-3'; GAPDH Fw 5'-ACTTTGGCATTGTGGAAGGG-3', Gapdh Rev 5'-CATGCCAGTGAGCTTCCCGTT-3'. Annealing was carried out at 58°C for all primer sets and up to 30 cycles were run for all amplifications except for Gapdh (23 cycles). Images were recorded with the Syngene G-box system (Syngene Bioimaging, Haryana, India) and intensities of the bands were quantitatively analysed using ImageJ Software (NIH, Bethesda, MD). Results represent the mean of at least three independent experiments and were normalized compared to the amount of housekeeping gene.

For RT-qPCR, cDNA was prepared using the High Capacity cDNA Reverse Transcription kit (Applied Biosystem); the RT-qPCR was performed using either Syber Green (Promega) or TaqMan Gene Expression (Applied Biosystem) master mix by Applied Biosystems 7500 Real-Time PCR. Primers list for Syber Green RT-qPCR:

Mef2c Fw 5'-CGATGCAGACGATTCAGTAG-3' and Mef2c Rev 5'-ACTGTTATGGCTGGACACTG-3'; Nkx2.5 Fw 5'-CAATGCCTATGGCTACAACG-3' and

Nkx2.5 Rev 5'-GCCAAAGTTCACGAAGTTGC-3'; Mhy7 Fw 5'AACTGGATGGTGACACGCAT-3' and Mhy7 Rev 5'-TGTGGTGGTTGAAGAACTGC-3'.

Forward primers sequences for TaqMan RT-qPCR:

PDE5A1: 5'-GACTGGGTGGAAGCGTG-3'

(Probe: 5'-GGATGATCACCGGGACTTT-3');

PDE5A2: 5'-AGAGTCTCCCGAGTCCAC-3'

(Probe: 5'-CCCACCTTTGCTATGTTGCCCTTTG-3');

PDE5A3: 5'-CAGTATCCTTTTCCTTCCTTCAAG-3'

(Probe: 5'-ACAGAGACATGGTCAACGCATGGT-3').

Reverse primer sequence for TaqMan RT-qPCR: 5'-GGATGCCTTCCTTGCACA-3'.

For quantification analysis, the comparative threshold cycle (Ct) method was used. The Ct values of each gene were normalized to the Ct value of Gapdh in the same RNA sample. The gene expression levels were evaluated by the fold change using the equation 2^{-ddCt}.

Western blot

Tissues were lysated in 50 mM Tris HCl pH 8, 150 mM NaCl, 1% w/v NP-40, 0.5% w/v sodium deoxycholate, 0.1% w/v sodium dodecyl sulphate, 0.5 v/v mM dithiothreitol, 10 mM β-glycerophosphate, 0.1 mM sodium vanadate, and protease inhibitor cocktail (Sigma-Aldrich, CA, USA) or in 20 mM Tris-HCl buffer pH 7.2 containing 0.2 mM EGTA, 5 mM β-mercaptoethanol, 2% v/v antiprotease cocktail (Sigma Aldrich, CA, USA), 1 mM PMSF, 5 mM $MgCl_2$, 0.1% v/v Triton X-100 and were electrophoresed in polyacrylamide gels and transferred onto polyvinylidene fluoride (PVDF) (Amersham, Piscataway, NY) membranes. Primary antibodies were incubated overnight at 4°C, and secondary antibodies were incubated 1 hour at room temperature. Blots were probed with rabbit polyclonal PDE5A (Santa Cruz, CA, USA) and mouse monoclonal β-TUBULIN (Sigma-Aldrich, CA, USA) antibodies. In the competition experiments 0.2 µg/ml PDE5A antibody was previously incubated with 40 µg/ml of recombinant PDE5A for 1 hour at room temperature. Signals were detected with horseradish peroxidase (HRP)-conjugated secondary antibodies and enhanced chemiluminescence (Santa Cruz Biotechnology, CA, USA). Chemiluminescent images of immunodetected bands were recorded with the Syngene G-box system (Syngene Bioimaging, Haryana, India) and immunoblot intensities were quantitatively analysed using ImageJ Software (NIH, Bethesda, MD). Results represent the mean of at least three independent experiments and were normalized to the amount of housekeeping proteins.

Immunofluorescence Analysis

Cells were fixed with ice cold 4% w/v paraformaldehyde in PBS and incubated for 10 minutes at 4˚C, washed 2 times with PBS to remove any paraformaldehyde residue and permeabilized with 0.1% v/v Triton®X-100 for 10 minutes at room temperature. Slides were then washed with PBS and incubated for 1 hour in 3% w/v BSA at room temperature. Primary antibodies (rabbit polyclonal PDE5A antibody, Abcam, UK, mouse monoclonal MHC antibody [MF20] from Hybridoma Bank and mouse monoclonal GFP antibody, SantaCruz Inc., CA, USA) were diluted in 1% w/v BSA and left overnight at 4˚C. After three washings for 10 minutes in PBS, coverslips were incubated with the appropriate secondary antibody fluorescently labeled (fluorescein isothiocyanate, FITC or Texas red; Pierce, IL, USA) for 1 hour at room temperature. Nuclei were stained with 4',6-diamidino-2-phenylindole (DAPI) (Life Technologies, CA, USA) and slides were finally mounted on microscope slides using MOWIOL® 4-88 reagent and left to dry for 1 hour then stored at 4˚C in the dark. Tissues were collected and fixed with 10% v/v Formalin for at least 24 hours at room temperature. Samples were dehydrated in an ascending series of alcohol concentrations (from 50% v/v to 100% v/v ethanol concentration) followed by toluene for a minimum of 4h. Tissues were placed in a bath of toluene paraffin for 2h in preparation for paraffin-embedding. The wax block was mounted on a microtome and sections of 5µm thickness were sliced. Slides were immersed in toluene for 20 minutes. Subsequently, the slides were rehydrated and then immersed in 2% v/v hydrogen peroxide/methanol solution for 20 minutes to block any endogenous peroxidase. Samples were examined by a Zeiss Axioskop2 plus microscope. Images were obtained with a Zeiss AxioCam HRc using the Axiovision software.

Confocal images were instead acquired using a 63X Zeiss oil immersion objective on a Zeiss Pascal LSM510 laser-scanning confocal microscope (Carl Zeiss). An argon laser was used to excite 488 nm fluorescently labeled secondary antibodies. Helium/neon lasers were used to excite 568 nm fluorescently labeled secondary antibodies. Zeiss Pascal software was used to gather image files.

Analysis of HL-1 size

Cell size quantification was performed 48 hours after transfection with PDE5A isoforms GFP-tagged vectors labeling actin microfilaments with Phalloidin–Tetramethylrhodamine B isothiocyanate (TRITC) (Sigma-Aldrich, CA, USA). Nuclei were stained with DAPI. Cell area (μm^2) or longitudinal and transversal axes length (µm) were measured using the software "Image J" (developed by USA National Institutes of Health). Images were acquired by Nikon Eclipse Ti-S microscope.

Subcellular fractionation

Cells were trypsinized, harvested, lysed in IB-1 buffer (225 mM mannitol, 75 mM sucrose, 0.1 mM EGTA and 30-mM Tris–HCl pH 7.4) and homogenized by a Teflon pestle. Homogenate was then centrifugated at 600g for 5 min at 4 °C to precipitate nuclei. The supernatant was centrifugated again at 7,000 g for 10 min at 4 °C to recover the cytosolic fraction containing lysosomes and microsomes (supernatant). LAMIN A/C (goat polyclonal, Santa Cruz, CA, USA) was used as a marker of nuclear fraction and GAPDH (rabbit polyclonal, Santa Cruz, CA, USA) or β-TUBULIN (mouse monoclonal, Sigma-Aldrich, CA, USA) as cytoplasmic markers.

Cell cycle

HL-1 and NIH3T3 cells were initially plated at a density of 5 x 10^5 cells/well in 3.5 cm dishes. Next day cells were transfected with PDE5A isoforms GFP-tagged vectors. Twenty four hours later, cells were synchronized with 0.5 mM L-Mimosine (Sigma-Aldrich, CA, USA). After 16 hrs, cells were washed with PBS and incubated in fresh culture media. At various times after release from the L-Mimosine block the cells were treated with trypsin, harvested, and centrifuged at 2000 g for 5 min. The pellets were washed with PBS and then centrifuged again. Cells were fixed with 1% w/v paraformaldehyde for 1hr at 4°C, then centrifuged for 5 min at 300 g; supernatant was removed by aspiration and pellets washed with PBS. For cell membrane solubilization, 1 ml 70% v/v ethanol was added to the cell pellet, and cell suspension incubated overnight at 4°C. Fixed cells were washed with PBS, centrifuged and incubated for 3 hr at room temperature with propidium iodide/RNAse A solution (PI, 50 µg/mL, Sigma-Aldrich, CA, USA), ribonuclease (1 mg/ml Sigma-Aldrich, CA, USA). The cell cycle distribution and DNA content were measured using a CyAn cytofluorimeter (Dako). 5 x 10^3 cells were counted for each sample. The percentage of cells in different phases of the cell cycle was analyzed by FlowJo (TreeStar, Ashland, OR, USA).

Statistical analysis

Data obtained are presented as the means ± SD and ± SEM from at least three separate experiments, each performed in triplicate. The significance of the data was analyzed using the Student's t-test for parametric data and the Mann–Whitney test with Bonferroni corrections for nonparametric data. $P < 0.05$ was considered statistically significant (*$P < 0.05$, **$P < 0.01$, ***$P < 0.001$).

RESULTS

Identification of mPDE5A isoforms

The protein sequences of PDE5A in different mammalian species were retrieved from GenBank and aligned to compare their expression pattern. This analysis showed that up to three PDE5A isoforms were identified in the different species **(Fig. S1A)**. All known PDE5As are encoded by a single gene and the different isoforms can be translated from alternative start sites, therefore each isoform usually possesses an unique N-terminal region. In mouse only one isoform was identified so far (Burns et al., 1996). To investigate the hypothesis that other PDE5A isoforms could be expressed in mouse tissues the NCBI *Mus Musculus* and *Homo Sapiens* genome sequences of the *Pde5a* locus were compared. The comparison between the mouse *Pde5a* first intron and the human gene revealed the presence of regions with a high homology degree [*hPDE5 (NC_018915.2) 120524928-120524828: m/PDE5 (NT_039240.7) 71815847-71815946; hPDE5 (NC_018915.2) 120516972-120516481/ mPDE5 (NT_039240.7) 71822133-71822269*]. This homology suggested that *mPde5a* gene may produce multiple protein isoforms. The first region of homology (Exon 1a) showed a newly identified potential start codon and the downstream sequence may encode 9 amino acids corresponding to the first exon of *hPDE5A2*. Similarly to the human gene, an in-frame ATG is within the second exon of the *mPde5a* gene which may represent an alternative translation start site for a third isoform. Since the comparative analysis of the sequences in the databank suggested that the murine gene can encode three PDE5A isoforms as the human gene, putative isoforms were named according to their equivalent human isoforms as mPDE5A1, mPDE5A2 and mPDE5A3. **Fig. 1A** shows the differences in N-terminal nucleotide sequence among the putative isoforms.

mPDE5A isoforms show similar biochemical features

To investigate the expression of *mPde5A* isoforms, total RNA from murine cardiomyocytes was extracted and retro-transcribed. *mPde5a1* and *mPde5a2* transcripts of expected size were detected as well as a band compatible for *mPde5a3* isoform at minor intensity (**Fig. S1B**). These results strongly suggest that three *mPde5a* isoforms are expressed in mice like in humans.

To evaluate the biochemical properties of the new putative identified mPDE5A isoforms, single isoform ORFs were obtained from a cDNA embryo library, cloned into pCDNA3.1 expression vector and then transfected into HEK293T cell line. Western blot analysis performed on cellular lysates of transfected cells showed cross-reaction between anti-PDE5A antibody and the cloned mPDE5A isoforms (**Fig. S1C**). Three bands of 99 ± 2.8 kDa, 91 ± 2.7 kDa and 89 ± 2.4 kDa were identified corresponding to mPDE5A1, mPDE5A2 and mPDE5A3, respectively. In the same

cellular lysates cGMP hydrolytic activity was assayed. In untransfected HEK293T cells a negligible level of endogenous cGMP-PDE activity was measured. Exogenous mPDE5A1 possess a Km higher than exogenous mPDE5A2 and mPDE5A3 (2.5 μM ± 0.5 for mPDE5A1, 0.75 μM ± 0.01 for mPDE5A2 and 1.06 μM ± 0.07 for mPDE5A3) indicating that mPDE5A1 is the isoform with the lowest affinity for cGMP (**Fig. 1B**). Since PDE5A is specifically inhibited by sildenafil at nanomolar concentrations (Ballard et al., 1998), an inhibition study was performed and demonstrated that all mPDE5A isoforms were inhibited by sildenafil with the same potency (IC_{50} 7.8 nM ± 1.11 for mPDE5A1, 5.2 nM ± 1.03 for mPDE5A2 and 4.7 nM ± 1.06 for mPDE5A3) (**Fig. 1C**).

In vivo expression of mPDE5A isoforms

To delineate the tissue distribution pattern of mPDE5A isoforms, a set of adult mouse organs was collected and PDE5A expression was analyzed both at mRNA and protein level.

RT-PCR analysis revealed the presence of amplified cDNA bands of the expected molecular sizes in all examined organs except for the liver. (**Figs. 1D**); in the heart, *mPde5a1* and *mPde5a2* mRNAs were expressed whereas *mPde5a3* mRNA was undetectable.

The expression of PDE5A isoforms in murine tissues was also examined by Western blot analysis and quantified by densitometry (**Fig. 1E)**. Since no specific antibodies for different PDE5A isoforms are currently available, a PDE5A pan antibody was used. PDE5A antibody identified protein bands which migrate as the recombinant mPDE5A isoforms **(Fig. S1C)**. A band with the highest apparent molecular weight corresponding to PDE5A1 (MW 99 ± 2.8 kDa) was expressed in brain, cerebellum, heart, lung and ovary; a band with an apparent molecular weight corresponding to PDE5A2 (MW 91 ± 2.7 kDa) was expressed in brain, cerebellum, heart, lung, and ovary; a band with an apparent molecular weight corresponding to PDE5A3 isoform (MW 89 ± 2.4 kDa) was expressed in kidney and testis. The same pattern of protein expression was obtained in the absence of protease inhibitors suggesting that the different bands detected by western blot are not due to proteolytic digestion (data not shown). Furthermore, to test the specificity of the detected bands a competition experiment was performed using a protein homogenate of lung and heart tissues **(Fig. S1D)**. Western blot analysis showed that the two bands of the apparent MW of 99 kDa and 91 kDa corresponding to PDE5A1 and PDE5A2 disappeared when the PDE5A antibody was incubated with purified recombinant PDE5A protein (**Fig. S1D**). Interestingly, the competition experiment revealed a further specific band at 104kDa in cerebellum, lung and ovary tissues **(Fig. S1D)**.

Taken together these data show that mouse tissues express at least three PDE5A isoforms and mPDE5A1 and mPDE5A2 are both expressed in mouse heart.

mPDE5A isoforms are differently expressed in heart and cardiomyocytes at different ages

Expression of *mPde5a* isoforms was further investigated by mRNA and protein analyses in isolated cardiomyocytes and hearts obtained from 13.5 days post coitum (dpc), neonatal and adult mice (**Figs. 2A-B**). As displayed in **Fig. 2A**, *mPde5a1* and *mPde5a2* mRNA expression levels were found similar in samples obtained from hearts of different ages; *mPde5a3* mRNA expression decreased with time becoming undetectable in adult heart. The mRNAs of the three isoforms were identified in samples obtained from cultured cardiomyocytes, indicating that *mPde5as* are specifically expressed in cardiomyocytes beside cells of different lineage. In particular, *mPde5a1* mRNA levels were lower in adult cardiomyocytes compared to cardiomyocytes isolated from embryos and neonatal mice. *mPde5a2* mRNA expression levels were the highest and not modified during cardiac development. *mPde5a3* mRNA expression levels gradually decreased and it was almost undetectable at the birth (**Fig. 2B**). Both *mPde5a1* and *mPde5a2* expression levels were recorded by real time PCR analyses in adult heart tissue and isolated cardiomyocytes **(Fig. S1E)**.

Due to the lack of specific antibodies for different PDE5A isoforms, neonatal and adult isolated cardiomyocytes were examined for total PDE5A localization by immunofluorescence analyses. Intracellular PDE5A expression pattern resulted in protein dispersion within the cytoplasm and in a localization at the z-lines (**Figs. 2C-D**). Interestingly, PDE5A nuclear localization was found both in neonatal and adult cardiomyocytes (**Figs. 2C-D**) which was confirmed through nucleus-cytosol fractionation experiments performed on cellular homogenates obtained from neonatal cardiomyocytes (**Fig. 2E**). To investigate if PDE5A nuclear localization occurs also in vivo, immunofluorescence analyses were performed on neonatal and adult heart sections, confirming nuclear and cytoplasmic localization of PDE5A at tissue level (**Figs. S2A-B)**.

mPDE5A isoforms are differently localized in HL-1 cells

Endogenous PDE5A distribution pattern was first investigated in cardiac HL-1 cell line (Claycomb et al., 1998; White et al., 2004) and confocal analysis revealed that PDE5A was localized both in the nucleus and cytoplasm (**Fig. 3A**). It has been shown for other PDEs that alternative N-terminal domains drives different cellular distribution (Houslay and Adams, 2003; Sonnenburg et al., 1995). To verify if the N-terminus differences of mPDE5A isoforms lead to different subcellular localization, GFP-tagged isoforms were transfected in the HL-1 cells (Fig. 3 and S2C). The overexpression of GFP-tagged mPDE5A isoforms revealed a prevalent cytoplasmic localization of

mPDE5A1 (**Fig. 3B**), whereas mPDE5A2 and mPDE5A3 showed both nuclear and cytoplasmic localization. Taking advantage of GFP co-expression it was possible to quantify that 13.5% of mPDE5A1 overexpressing cells showed a PDE5A nuclear localization, whereas cells overexpressing mPDE5A2 and mPDE5A3 display a more frequent PDE5A nuclear localization (37.3% and 30.1%, respectively). Subcellular fractionation experiments confirmed that PDE5A is present both in the nucleus and cytoplasm of HL-1 cells (**Fig. 3C**)**.**

Taken together these data suggest that PDE5A localizes also within the nucleus and this event occurs more frequently for mPDE5A2 and mPDE5A3 isoform.

mPDE5A isoforms overexpression accelerates cell cycle and increases polyploidy of HL-1 cells

No data are available on the specific role of PDE5A isoforms in the different tissues and how their expression can selectively modulate cell growth and differentiation. Indeed PDE5A suppression inhibits cell growth of cancer cells (Zhu et al., 2005). The effects of mPDE5A isoform overexpression was investigated in HL-1 cell cycle (**Fig. 4A**). GFP and mPDE5As-GFP overexpressing cells were synchronized and arrested in G1 phase by L-Mimosine treatment. After the removal of L-Mimosine, the percentage of cells in S phase increased in all samples. The percentage of HL-1 cells in S phase was slightly higher in mPDE5A isoforms overexpressing cells compared to control cells, even if it was not statistically significant. The percentage of cells in G2 was higher 24 hours after L-Mimosine removal for all mPDE5A isoforms, suggesting an acceleration of the cell cycle (**Fig. 4A**).

In G2 phase, cells contain the double of DNA content than in G1 phase. To assess the polyploidy degree of mPDE5A overexpressing cardiomyocytes, flow cytometry analysis of HL-1 cells overexpressing mPDE5A isoforms was performed. A significant increase of the percentage of polyploid cells (> 4N) was found in HL-1 cells overexpressing mPDE5A1 and mPDE5A3 (6.2% ± 1.1 and 8.3% ± 0.9, respectively) compared to control cells (4.3% ± 0.7) whereas mPDE5A2 overexpression did not trigger any significant change in the percentage of polyploid cells (3.2% ± 0.5) (**Fig. 4B**).

No differences in the specific activities were recorded between GFP-tagged and untagged isoforms indicating that the effects on cell cycle and polyploidy were due the intrinsic properties of the different PDE5A isoforms (**Fig. S2D**).

These results indicate that mPDE5As overexpression triggers cell cycle progression and mPDE5A1 and mPDE5A3 overexpression increases cardiomyocyte polyploidy.

mPDE5A isoforms overexpression induces cardiac hypertrophy

The increase of the nuclear DNA content per cell could be due to the entrance of the cells in mitosis but in the case of cardiomyocytes it could be due to the presence of two nuclei per cell, which are associated to hypertrophy of cardiomyocytes (Ahuja et al., 2007; Liu et al., 2010). Several studies performed in humans and mice suggest an important role of PDE5A expression in the establishment of cardiac hypertrophy in pathological conditions (Pokreisz et al., 2009; Zhang et al., 2010), event that is accompanied by an increase of the polyploidy of cardiomyocytes (Ahuja et al., 2007; Liu et al., 2010).

To investigate if the increase of polyploid cells correlates with an increase of nuclei number per cell, the percentage of binucleated cardiomyocytes was evaluated by immunofluorescence staining of HL-1 cells overexpressing mPDE5A isoforms. In HL-1 control cells the binucleated cells were estimated to be 14.3% ± 3.5 of total GFP positive cells; mPDE5A1 overexpression almost doubled the percentage of binucleated cells (30.4% ± 5.1); mPDE5A2 overexpression increased the percentage of binucleated cell to a minor extent (22.6% ± 3.2) whereas mPDE5A3 overexpression was the most efficient to increase the number of binucleated cells (33.5% ± 5.2) (**Fig. 4C**).

The increase of cell size is considered a marker of cardiomyocyte hypertrophy (Sadoshima and Izumo, 1997; Ahuja et al., 2007). For this reason cell area of HL-1 overexpressing mPDE5A isoforms was measured. Interestingly, only overexpression of mPDE5A3 but not mPDE5A1 and mPDE5A2 significantly increased HL-1 cells area (**Fig. 4D**). This result was confirmed through the measurement of longitudinal and transversal axes length of HL-1 cells overexpressing mPDE5A isoforms (**Figs. S2E-F**). In particular, mPDE5A3 significantly increased the length of transversal axis suggesting that this isoform could promote cell hypertrophy through specific rearrangement of cell shape (**Fig. S2F**). Furthermore RT-qPCR analysis revealed that hypertrophic markers were induced by PDE5A isoform overexpression (**Fig. 4E)**. Notably, PDE5A3 was able to up-regulate all markers tested, confirming its potential role on HL-1 hypertrophy instauration (**Fig. 4E)**.

Overall these results suggest that mPDE5A1 and mPDE5A3 are the isoforms that prevalently increase DNA content and nuclei number per cell whereas, in addition, mPDE5A3 overexpression is able to enhance cell area by increasing cellular width.

DISCUSSION

Multiple isoforms of PDE5A were described in different species, e.g. three isoforms in humans, two isoforms in rats and dogs (Lin et al., 2000b; Lin et al., 2003) and only one in mouse (Burns et al., 1996). The presence of additional PDE5A isoforms in mouse was not further investigated even if Giordano and co-workers suggested the presence of different PDE5A isoforms in murine neuroblastoma N18TG2 cell line and in some murine tissues (Giordano et al., 2001).

This study reports for the first time the identification and functional characterization of three different PDE5A isoforms in *M. Musculus*. mPDE5A1 showed the highest Km value, whereas all mPDE5A isoforms were similarly inhibited by sildenafil. We further examined the distribution of the new identified isoforms across tissues, their subcellular distribution, as well as functional and expressional regulation in physiological conditions. As a final outcome, the biological role of each isoform was investigated. RT-PCR analysis revealed a noticeably distinct distribution pattern for all mPDE5A isoforms among various mouse tissues. *mPde5a1* and *mPde5a2* were expressed at high levels in the lung, which can be in line with the primary role of PDE5A in vaso-constricting the pulmonary vasculature and its involvement in pulmonary hypertension (Hemnes and Champion, 2006). In adult heart, *mPde5a1* and *mPde5a2* mRNAs were expressed whereas *mPde5a3* was barely present. To be note that in adult heart PDE5A levels are relatively low and barely detectable in physiological conditions and they became elevated during hypertrophy (Nagendran et al., 2007).

Protein distribution of the three isoforms was also assessed and it was found similar to our previous observations (Giordano et al., 2001). In brain, cerebellum, heart, lung and ovary two bands were clearly visible, the most intense corresponding, on the base of MW (99 ± 2.8 kDa), to the mPDE5A1 cloned isoform; the other band, of lower intensity, had the same MW (91 ± 2.7 kDa) of mPDE5A2 cloned isoform. Moreover, some tissues displayed a band of higher MW (104 ± 2.7 kDa) respect to mPDE5A1, this band is specific as evaluated by competition experiments and it could represent a post-translational modification of mPDE5A isoforms. In brain and heart the presence of mPDE5A1 was evident, whereas the expression of mPDE5A2 isoform was barely detectable even if *mPde5a2* mRNA was detected. It is still to understand why the protein is not translated. A band of 89 ± 2.4 kDa MW, corresponding to mPDE5A3, was detected only in testis and in kidney. In these two organs and in liver, an immunoreactive band of 96 ± 2.7 kDa MW between mPDE5A1 and mPDE5A2 isoforms was also detected. Similarly to PDE5A1 and PDE5A2 expression in human (Lin et al., 2000a), mPDE5A1 and mPDE5A2 were expressed in all tissues analyzed except for liver. mRNA of *mPde5a3* was found in several tissues but without the

corresponding protein expression suggesting that mPDE5A3 could be not translated or, alternatively, rapidly degraded.

To further characterize regulation, catalytic activity, drugs sensitivity and subcellular localization of each isoform, exogenously expressed mPDE5A isoforms were transfected into HEK293T cell line. We observed that all three PDE5A isoforms possess similar substrate affinity (mPDE5A1 possess a Km higher than exogenous mPDE5A2 and mPDE5A3, indicating that this is the isoform with the lowest affinity for cGMP) and sildenafil sensitivity. This is in agreement with previous reports in which PDE5A human isoforms were tested for their cGMP-catalytic activity and sildenafil sensitivity showing that human PDE5A1 possess a Km and IC_{50} higher than human PDE5A2 and PDE5A3 (Lin et al., 2000a).

It is likely that in various tissues and cell types the distinct N-termini of the three isoforms might endow them with specific regulatory properties, as well as specific subcellular localization. To assess this possibility the localization of the endogenous PDE5A in HL-1 cells was examined. The main compartments in which PDE5A was detected by immunofluorescence were: subsarcolemmal region, nucleus and myofilaments. Sarcomeric localization of PDE5A was extensively investigated in literature (Nagayama et al., 2008; Pokreisz et al., 2009; Takimoto et al., 2005). On z-lines, PDE5A is likely to be responsible of the regulation of a cGMP pool which, by PKG activation and consequent phosphorylation of Troponin I, should desensitize myofilaments to Ca2+, thus antagonizing the β-adrenergic stimulated inotropic effect (Lee et al., 2010; Senzaki et al., 2001). In the sarcoplasmatic reticulum, PDE5A might interacts with proteins involved in Ca^{2+} storing, as already reported by Wilson et al. (2008), where, controlling cGMP levels, should coordinate Ca^{2+} release (Wilson et al., 2008). In a recent work, however, Lee and co-workers (2015) showed that PDE9 but not PDE5 co-localizes with sarcoplasmic reticulum ATPase-2a (Lee et al., 2015). We and others reported a subsarcolemmal localization of PDE5A in cardiomyocytes (Isidori et al., 2015; Takimoto et al., 2005); indeed, it has been hypothesized that the subsarcolemmal pool of cGMP was under the exclusive control of PDE2 (Castro et al., 2006; Polito et al., 2013). Our observations could overturn the previous knowledge about phosphodiesterases targeting to that compartment. An unexpected cellular compartment that show a strong positivity for PDE5A was the nucleus, both in neonatal and adult cardiomyocytes and in HL-1 cell line, either by immunofluorescence and fractionation analyses. A nuclear localization in cardiomyocytes for this enzyme has never been described before, even though nuclear staining was shown in some papers (Lee et al., 2015) and a nuclear translocation of PKG was already demonstrated (Chen and Roberts, 2014). The sarcomeric and nuclear subcellular localization of endogenous PDE5A was also validated on neonatal and adult

hearts. In neonatal mice, the nuclear compartmentalization of PDE5A resulted less evident than adult hearts in which the percentage of PDE5A positive nuclei is less than 20%.

One limitation for this study is the lack of specific antibodies for the three isoforms. The main hurdle to obtain specific antibodies is due to the overlapping coding sequences of PDE5A isoforms. We will attempt to develop specific antibodies directed against the three PDE5A isoforms by different strategies to further investigate their specific compartmentalization. In the meanwhile, to identify mPDE5A isoforms localization, cardiac HL-1 cells were transfected with constructs containing mPDE5A isoforms fused to a GFP-tag, allowing to visualize the transfected isoforms in distinct compartments. This cellular system is low transfectable but is the only available cell line of cardiac origin. A different subcellular distribution among the three isoforms was revealed; in particular mPDE5A1 resulted to be mainly localized in the cytoplasm, whereas mPDE5A2 and mPDE5A3 showed also an evident nuclear localization.

Increased expression of PDE5A was reported in pathological conditions such as cancer progression (Sponziello et al., 2015; Tiwari and Chen, 2013), but no data are available of the effect of increased intracellular level of PDE5A on cell cycle and cell growth.

To investigate mPDE5A isoforms specific role, the effects induced by exogenous overexpression of each variant were evaluated on cell cycle and cell growth. The overexpression of the three isoforms induced a sustained cell cycle progression in cardiomyocytes (HL-1) and fibroblasts (NIH3T3) transfected cells (Fig. 4A and Fig. S2G), an effect that was not affected by PDE5A pharmacological inhibition (data not shown). The persistence of the effect on the cell cycle of PDE5A overexpression in the presence of PDE5A specific inhibitors suggests that it could be due to an intrinsic structural property of the protein. Indeed in smooth muscle cells PDE5A localizes at the level of centrosomes allowing to hypothesize that it could play an important structural role in the assembly of the mitotic spindle and, therefore, in the regulation of cell cycle progression (Dolci et al., 2006).

In HL-1, overexpression of mPDE5A isoforms induced an increase of cells in G2 phase respect to mock cells, event associated to increased proliferation or to a G2 arrest. Indeed, HL-1 transfected with mPDE5A isoforms had a double content of DNA and double nuclei. Cardiomyocytes binucleation is considered a marker of hypertrophy (Nagendran et al., 2007). Also in our experiments the binucleation was accompanied by an increase in cell area following mPDE5A3 isoform overexpression. Indeed, mPDE5A3 overexpression widen HL-1 area and transversal axis length up to 20% respect to control cells and induced hypertrophic markers unrevealing a potential role of this isoform in cardiac hypertrophy. This is in line with mRNA expression analysis showing

that *mPde5a3* is downregulated in mouse heart and cardiomyocytes during the life in physiological conditions.

In vitro and in vivo data indicate PDE5A3 increases in pathological cardiac conditions (manuscript in preparation). The understanding of the regulation of mPDE5A isoforms, their expression and activity in relation to their cellular context constitute an important step toward the improvement of the diagnostic, prognostic, and predictive values of PDE5A in heart disease or more widely in PDE5A-related diseases.

ACKNOWLEDGMENTS

We thank Dr. Fabrizio Padula (Dept. DAHFMO Sapienza University, Rome, Italy) for FACS analyses, Dr. Rita Assenza, (Dept. DAHFMO Sapienza University, Rome, Italy) and Dr. Roberto Gimmelli (Dept. Experimental Medicine, Sapienza University, Rome, Italy) for technical support.

Conflict of Interest Disclosure: None

REFERENCES

Ahuja P, Sdek P, MacLellan WR. 2007. Cardiac myocyte cell cycle control in development, disease, and regeneration. Physiological Reviews 87: 521-544.

Ballard SA, Gingell CJ, Tang K, Turner LA, Price ME, Naylor AM. 1998. Effects of sildenafil on the relaxation of human corpus cavernosum tissue in vitro and on the activities of cyclic nucleotide phosphodiesterase isozymes. The Journal of Urology 159: 2164-2171.

Burns F, Zhao AZ, Beavo JA. 1996. Cyclic nucleotide phosphodiesterases: gene complexity, regulation by phosphorylation, and physiological implications. Adv Pharmacol 36: 29-48.

Castro LR, Verde I, Cooper DM, Fischmeister R. 2006. Cyclic guanosine monophosphate compartmentation in rat cardiac myocytes. Circulation 113: 2221-2228.

Catalano S, Campana A, Giordano C, Gyorffy B, Tarallo R, Rinaldi A, Bruno G, Ferraro A, Romeo F, Lanzino M, Naro F, Bonofiglio D, Ando S, Barone I. 2016. Expression and Function of Phosphodiesterase Type 5 in Human Breast Cancer Cell Lines and Tissues: Implications for Targeted Therapy. Clinical Cancer Research 22: 2271-2282.

Chen J, Roberts JD, Jr. 2014. cGMP-dependent protein kinase I gamma encodes a nuclear localization signal that regulates nuclear compartmentation and function. Cellular Signalling 26: 2633-2644.

Claycomb WC, Lanson NA, Jr., Stallworth BS, Egeland DB, Delcarpio JB, Bahinski A, Izzo NJ, Jr. 1998. HL-1 cells: a cardiac muscle cell line that contracts and retains phenotypic characteristics of the adult cardiomyocyte. Proceedings of the National Academy of Sciences of the United States of America 95: 2979-2984.

Conti M, Beavo J. 2007. Biochemistry and physiology of cyclic nucleotide phosphodiesterases: essential components in cyclic nucleotide signaling. Annual Review of Biochemistry 76: 481-511.

Dolci S, Belmonte A, Santone R, Giorgi M, Pellegrini M, Carosa E, Piccione E, Lenzi A, Jannini EA. 2006. Subcellular localization and regulation of type-1C and type-5 phosphodiesterases. Biochemical and Biophysical Research Communications 341: 837-846.

Giordano D, De Stefano ME, Citro G, Modica A, Giorgi M. 2001. Expression of cGMP-binding cGMP-specific phosphodiesterase (PDE5) in mouse tissues and cell lines using an antibody against the enzyme amino-terminal domain. Biochimica et Biophysica Acta 1539: 16-27.

Goldstein I, Lue TF, Padma-Nathan H, Rosen RC, Steers WD, Wicker PA. 1998. Oral sildenafil in the treatment of erectile dysfunction. Sildenafil Study Group. The New England Journal of Medicine 338: 1397-1404.

Hemnes AR, Champion HC. 2006. Sildenafil, a PDE5 inhibitor, in the treatment of pulmonary hypertension. Expert Review of Cardiovascular Therapy 4: 293-300.

Houslay MD, Adams DR. 2003. PDE4 cAMP phosphodiesterases: modular enzymes that orchestrate signalling cross-talk, desensitization and compartmentalization. The Biochemical Journal 370: 1-18.

Isidori AM, Cornacchione M, Barbagallo F, Di Grazia A, Barrios F, Fassina L, Monaco L, Giannetta E, Gianfrilli D, Garofalo S, Zhang X, Chen X, Xiang YK, Lenzi A, Pellegrini M, Naro F. 2015. Inhibition of type 5 phosphodiesterase counteracts beta2-adrenergic signalling in beating cardomyocytes. Cardiovascular Research 106: 408-420.

Kotera J, Fujishige K, Akatsuka H, Imai Y, Yanaka N, Omori K. 1998. Novel alternative splice variants of cGMP-binding cGMP-specific phosphodiesterase. The Journal of Biological Chemistry 273: 26982-26990.

Kotera J, Fujishige K, Omori K. 2000. Immunohistochemical localization of cGMP-binding cGMP-specific phosphodiesterase (PDE5) in rat tissues. The Journal of Histochemistry and Cytochemistry 48: 685-693.

Lee DI, Vahebi S, Tocchetti CG, Barouch LA, Solaro RJ, Takimoto E, Kass DA. 2010. PDE5A suppression of acute beta-adrenergic activation requires modulation of myocyte beta-3 signaling coupled to PKG-mediated troponin I phosphorylation. Basic Research in Cardiology 105: 337-347.

Lee DI, Zhu G, Sasaki T, Cho GS, Hamdani N, Holewinski R, Jo SH, Danner T, Zhang M, Rainer PP, Bedja D, Kirk JA, Ranek MJ, Dostmann WR, Kwon C, Margulies KB, Van Eyk JE, Paulus WJ, Takimoto E, Kass DA. 2015. Phosphodiesterase 9A controls nitric-oxide-independent cGMP and hypertrophic heart disease. Nature 519: 472-476.

Lin CS, Lau A, Tu R, Lue TF. 2000a. Expression of three isoforms of cGMP-binding cGMP-specific phosphodiesterase (PDE5) in human penile cavernosum. Biochemical and Biophysical Research Communications 268: 628-635.

Lin CS, Lau A, Tu R, Lue TF. 2000b. Identification of three alternative first exons and an intronic promoter of human PDE5A gene. Biochemical and Biophysical Research Communications 268: 596-602.

Lin CS, Lin G, Lue TF. 2003. Isolation of two isoforms of phosphodiesterase 5 from rat penis. International Journal of Impotence Research 15: 129-136.

Lin CS, Lin G, Xin ZC, Lue TF. 2006. Expression, distribution and regulation of phosphodiesterase 5. Current Pharmaceutical Design 12: 3439-3457.

Liu Z, Yue S, Chen X, Kubin T, Braun T. 2010. Regulation of cardiomyocyte polyploidy and multinucleation by CyclinG1. Circulation Research 106: 1498-1506.

Lukowski R, Krieg T, Rybalkin SD, Beavo J, Hofmann F. 2014. Turning on cGMP-dependent pathways to treat cardiac dysfunctions: boom, bust, and beyond. Trends in Pharmacological Sciences 35: 404-413.

Nagayama T, Zhang M, Hsu S, Takimoto E, Kass DA. 2008. Sustained soluble guanylate cyclase stimulation offsets nitric-oxide synthase inhibition to restore acute cardiac modulation by sildenafil. The Journal of Pharmacology and Experimental Therapeutics 326: 380-387.

Nagendran J, Archer SL, Soliman D, Gurtu V, Moudgil R, Haromy A, St Aubin C, Webster L, Rebeyka IM, Ross DB, Light PE, Dyck JR, Michelakis ED. 2007. Phosphodiesterase type 5 is highly expressed in the hypertrophied human right ventricle, and acute inhibition of phosphodiesterase type 5 improves contractility. Circulation 116: 238-248.

Pokreisz P, Vandenwijngaert S, Bito V, Van den Bergh A, Lenaerts I, Busch C, Marsboom G, Gheysens O, Vermeersch P, Biesmans L, Liu X, Gillijns H, Pellens M, Van Lommel A, Buys E, Schoonjans L, Vanhaecke J, Verbeken E, Sipido K, Herijgers P, Bloch KD, Janssens SP. 2009. Ventricular phosphodiesterase-5 expression is increased in patients with advanced heart failure and contributes to adverse ventricular remodeling after myocardial infarction in mice. Circulation 119: 408-416.

Polito M, Klarenbeek J, Jalink K, Paupardin-Tritsch D, Vincent P, Castro LR. 2013. The NO/cGMP pathway inhibits transient cAMP signals through the activation of PDE2 in striatal neurons. Frontiers in Cellular Neuroscience 7: 211.

Sadoshima J, Izumo S. 1997. The cellular and molecular response of cardiac myocytes to mechanical stress. Annu Rev Physiol 59: 551-571.

Senzaki H, Smith CJ, Juang GJ, Isoda T, Mayer SP, Ohler A, Paolocci N, Tomaselli GF, Hare JM, Kass DA. 2001. Cardiac phosphodiesterase 5 (cGMP-specific) modulates beta-adrenergic signaling in vivo and is down-regulated in heart failure. FASEB Journal 15: 1718-1726.

Shan X, Margulies KB. 2011. Differential regulation of PDE5 expression in left and right ventricles of feline hypertrophy models. PloS ONE 6: e19922.

Shimizu-Albergine M, Rybalkin SD, Rybalkina IG, Feil R, Wolfsgruber W, Hofmann F, Beavo JA. 2003. Individual cerebellar Purkinje cells express different cGMP phosphodiesterases (PDEs): in vivo phosphorylation of cGMP-specific PDE (PDE5) as an indicator of cGMP-dependent protein kinase (PKG) activation. The Journal of Neuroscience 23: 6452-6459.

Sonnenburg WK, Seger D, Kwak KS, Huang J, Charbonneau H, Beavo JA. 1995. Identification of inhibitory and calmodulin-binding domains of the PDE1A1 and PDE1A2 calmodulin-stimulated cyclic nucleotide phosphodiesterases. The Journal of Biological Chemistry 270: 30989-31000.

Sponziello M, Verrienti A, Rosignolo F, De Rose RF, Pecce V, Maggisano V, Durante C, Bulotta S, Damante G, Giacomelli L, Di Gioia CR, Filetti S, Russo D, Celano M. 2015. PDE5 expression in human thyroid tumors and effects of PDE5 inhibitors on growth and migration of cancer cells. Endocrine 50: 434-441.

Takimoto E, Champion HC, Belardi D, Moslehi J, Mongillo M, Mergia E, Montrose DC, Isoda T, Aufiero K, Zaccolo M, Dostmann WR, Smith CJ, Kass DA. 2005. cGMP catabolism by phosphodiesterase 5A regulates cardiac adrenergic stimulation by NOS3-dependent mechanism. Circulation Res 96: 100-109.

Thompson WJ, Appleman MM. 1971. Multiple cyclic nucleotide phosphodiesterase activities from rat brain. Biochemistry 10: 311-316.

Tiwari AK, Chen ZS. 2013. Repurposing phosphodiesterase-5 inhibitors as chemoadjuvants. Frontiers in Pharmacology 4: 82.

Tsai EJ, Kass DA. 2009. Cyclic GMP signaling in cardiovascular pathophysiology and therapeutics. Pharmacology & Therapeutics 122: 216-238.

White SM, Constantin PE, Claycomb WC. 2004. Cardiac physiology at the cellular level: use of cultured HL-1 cardiomyocytes for studies of cardiac muscle cell structure and function. American Journal of Physiology Heart and Circulatory Physiology 286(3):H823-829.

Yanaka N, Kotera J, Ohtsuka A, Akatsuka H, Imai Y, Michibata H, Fujishige K, Kawai E, Takebayashi S, Okumura K, Omori K. 1998. Expression, structure and chromosomal localization of the human cGMP-binding cGMP-specific phosphodiesterase PDE5A gene. FEBS 255: 391-399.

Zhang M, Takimoto E, Hsu S, Lee DI, Nagayama T, Danner T, Koitabashi N, Barth AS, Bedja D, Gabrielson KL, Wang Y, Kass DA. 2010. Myocardial remodeling is controlled by myocyte-targeted gene regulation of phosphodiesterase type 5. Journal of the American College of Cardiology 56:2021-2030.

Zhu B, Vemavarapu L, Thompson WJ, Strada SJ. 2005. Suppression of cyclic GMP-specific phosphodiesterase 5 promotes apoptosis and inhibits growth in HT29 cells. Journal of Cellular Biochemistry 94(2):336-350.

FIGURE LEGENDS

Figure 1. mPDE5A isoforms identification, expression and activity.

A. Nucleotide and amino acid sequences of mPDE5A isoforms showing alternative methionine (in bold) and the predicted molecular weight. Unique N-terminal sequence are underlined.

B. Lineweaver-Burk plot of phosphodiesterase activity (1/pmoles cGMP hydrol./min/ml) of mPDE5A single isoforms assayed using different cGMP substrate concentrations. The Michaelis constant (Km) for each mPDE5A isoform was calculated. Data represent the mean of three determinations ± SD.

C. Inhibition curve of mPDE5A single isoforms with sildenafil assayed through the cGMP hydrolysis radioactive assay. The assay was performed using 1μM cGMP as substrate concentration. The IC_{50} for each mPDE5A isoform was calculated. Data represent the mean of three different determinations ± SD.

D. Representative image of RT-PCR analysis performed on cDNA from several mouse tissues showing a different distribution of the three Pde5A murine isoforms. Samples were normalized assaying the expression of Gapdh.

E. Representative image of western blot on different mouse tissues (left panel). A PDE5A specific antibody was used to detect the presence of different PDE5A isoforms. TUBULIN was used as loading control. Molecular weights (kDa) of the observed bands are shown on blot right side with murine PDE5A isoforms; predicted molecular weights are shown in bold. Three determinations were performed on tissues from different mice.

Densitometric analysis of western blot (right panel). Samples were normalized assaying the expression of TUBULIN. Data represent the mean of three determinations ± SD.

Figure 2. mPDE5A isoforms expression in the heart.

A. Semi-quantitative RT-PCR performed on cDNA from total heart at different ages showing the relative abundance of each murine Pde5A isoform. Samples were normalized assaying the expression of Gapdh. Data represent the mean of three determinations performed in separate preparations ± SD. All p values were calculated using the Mann-Whitney test with Bonferroni corrections. * $P < 0.05$ and ** $P < 0.01$.

B. Semi-quantitative RT-PCR performed on cDNA from isolated cardiomyocytes at different ages showing the relative abundance of each murine Pde5A isoform. Samples were normalized assaying

the expression of Gapdh. Data represent the mean of three determinations performed in separate preparations ± SD.

C. Immunofluorescence analysis on isolated neonatal cardiomyocytes from at least three different preparations showing PDE5A localization (green) and sarcomeres (MF20; red). Nuclei were stained with DAPI (blue). Scale bar = 10 μm.

D. Immunofluorescence analysis on isolated adult cardiomyocytes from at least three different preparations showing PDE5A localization (green) and sarcomeres (MF20; red). Nuclei were stained with DAPI (blue). Scale bar = 30 μm.

E. Western blot analysis on nucleus/cytosol fractions of isolated neonatal cardiomyocytes stained with PDE5A antibody showing the subcellular localization of endogenous PDE5A. Antibodies against LAMIN and GAPDH were used to distinguish nuclear and cytosolic fractions respectively. 20-30μg of each fraction were loaded. At least three determinations were performed.

Figure 3: mPDE5A isoforms display different subcellular localization in HL-1 cells.

A. Confocal analysis on HL-1 cell lines showing endogenous PDE5A subcellular localization (green) and MF20 positivity (red). Nuclei were stained with DAPI. Three determinations were performed. Scale bar = 25 μm.

B. Analysis of HL-1 after 48 hours transfection with GFP-tagged PDE5A single isoforms revealing a predominant cytoplasmic localization of PDE5A1 and a nuclear and cytoplasmic localization of PDE5A2 and PDE5A3 isoforms. Nuclei were stained with DAPI. Three determinations were performed. Scale bar = 10 μm.

C. Western blot analysis on nucleus/cytosol fractions of HL-1 cells stained with PDE5A antibody; antibodies against LAMIN and TUBULIN were used to distinguish nuclear and cytosolic fractions, respectively. 30μg of each fraction were loaded. Three determinations were performed.

Figure. 4: mPDE5A isoform overexpression induces cell cycle progression and increases HL-1 cells cell size.

A. Flow Cytometry analysis of HL-1 cell cycle after 24 hours transfection with GFP-tagged PDE5A isoforms. DNA content was measured by cell cycle synchronization with L-Mimosine and PI staining. Cell cycle was evaluated at different time point (T0, T4, T8 and T24) corresponding to hours after L-Mimosine removal from cell cultures. Bar graphs represent the percentage of cells in G1 phase (left panel), S phase (middle panel) and G2 phase (right panel). Diagram represents the

mean of three independent experiments ± SD. All p values were calculated using the Mann–Whitney test with Bonferroni corrections. * $P < 0.05$ and ** $P < 0.01$.

B. Flow Cytometry analysis of cellular ploidy of HL-1 cells after 48 hours transfection with GFP-tagged PDE5A isoforms (left panel). Diagram (right panel) represents the percentage of haploid (2N), diploid (4N), or polyploid (>4N) according to PI staining. Data represents the mean of three independent experiments ± SD. All p values were calculated using the Mann-Whitney test with Bonferroni corrections. *$P < 0.05$, **$P < 0.01$ and ***$P < 0.001$.

C. Analysis of cellular ploidy of HL-1 cells after 48 hrs transfection with GFP-tagged PDE5A isoforms. Diagram represents the percentage of cells with 1-4 nuclei stained with DAPI. Ten fields (approximately 10 cells/field) from each sample were randomly selected and the number of nuclei/GFP positive cells was determined. Data represents the mean of three independent experiments ± SD. All p values were calculated using a the Mann–Whitney test with Bonferroni corrections. *$P < 0.05$, **$P < 0.01$ and ***$P < 0.001$.

D. Analysis of HL-1 area. Ten fields (approximately 10 cells/field) from each sample were randomly selected and the areas (μm^2) of GFP-positive cells were measured by ImageJ Software. Diagram represents the mean of three independent experiments ± SD. All p value were calculated using a the Mann–Whitney test with Bonferroni corrections. *$P < 0.05$.

E. RT-qPCR analysis of HL-1 cells after 48 hrs transfection with GFP-tagged PDE5A isoforms. Myosin heavy chain 7 (myh7), myocytes-specific enhancer factor 2C (Mef2C) and NK2 homeobox 2.5 (Nkx2.5) were used as hypertrophic markers. Data are reported as fold change versus mock HL-1 cells. Gapdh was used as loading control. Data represents the mean of three independent experiments ± SD. All p values were calculated using a the Mann–Whitney test with Bonferroni corrections. *$P < 0.05$, **$P < 0.01$ and ***$P < 0.001$.

A

Name	Unique N-terminal nucleotide coding sequence	Amino-acid sequence (with alternative Met in bold)	Predicted molecular weight (kDa)
PDE5A1	Atggaacgagcgggccccaac tccgtgcggtcgcagcagcagc gggacccggactgggtggaag cgtggctggatgatcaccggga ctttaccttctcttactttattaga aaggccaccagagac	MERAGPNSVRSQQQRDP DWVEAWLDDHRDFTFSYF IRKATRDMVNAWFSE	98
PDE5A2	Atgttgccctttggagacaaaa cgagggac	MLPFGDKTRDMVNAWFSE	94
PDE5A3	/	MVNAWFSE	93

B

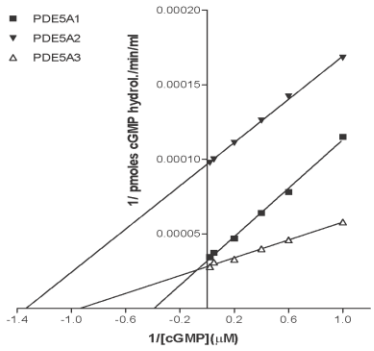

C

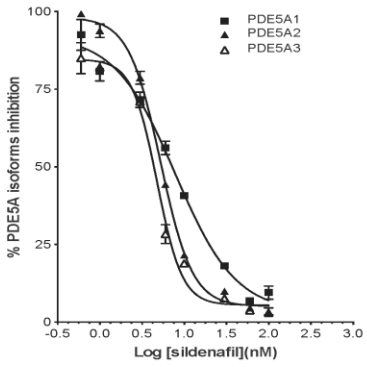

D

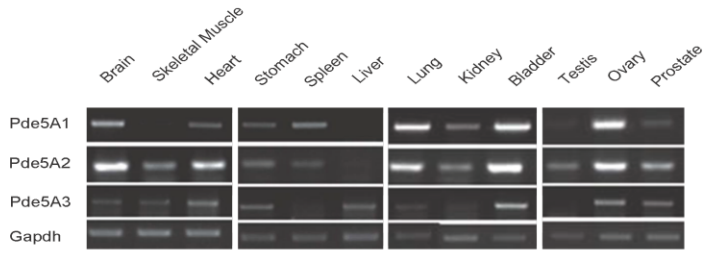

E

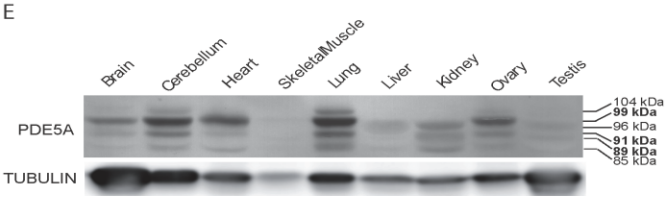

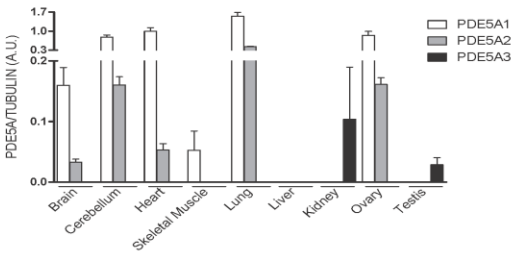

Figure 1

Figure 1

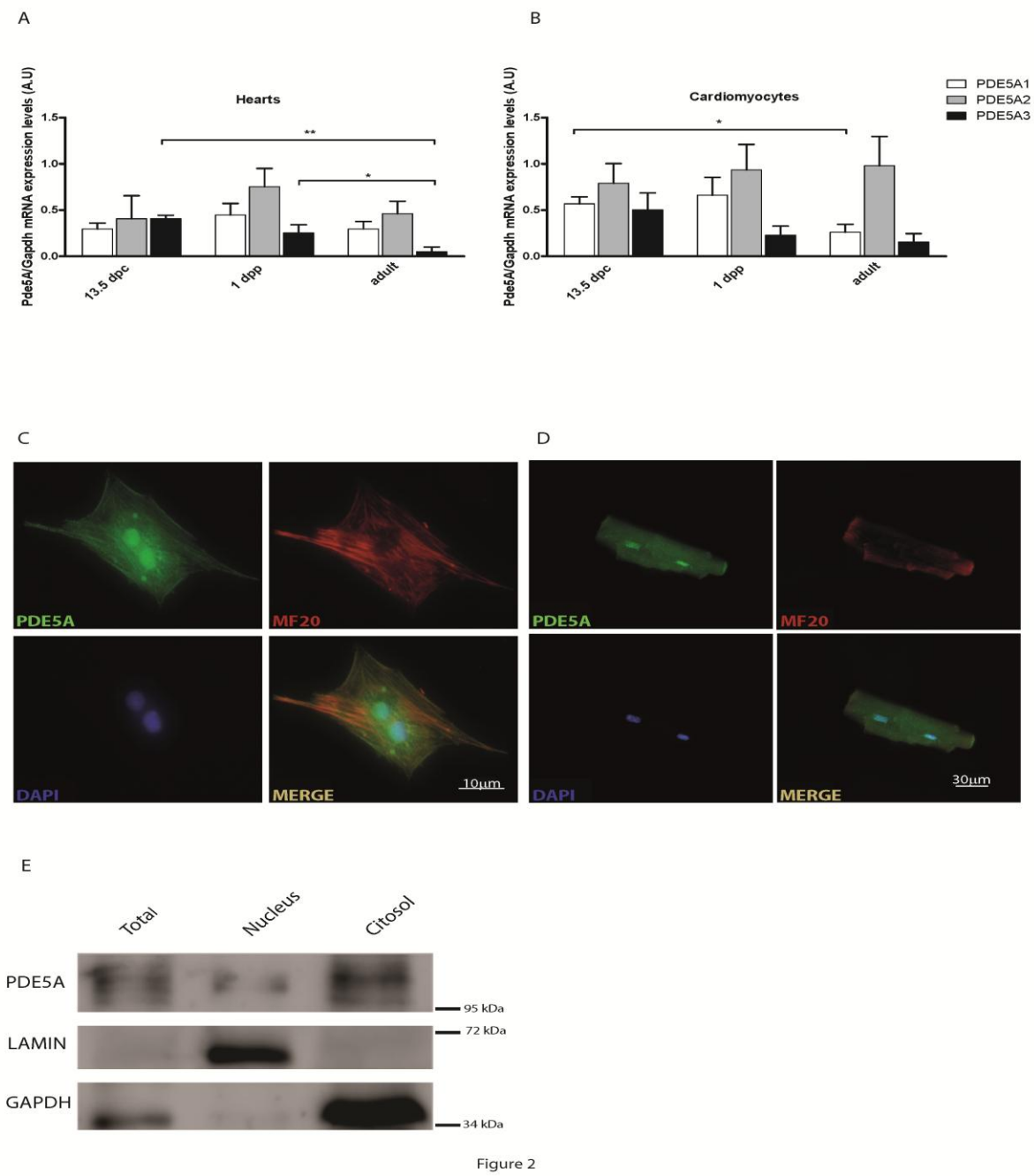

Figure 2

Figure 2

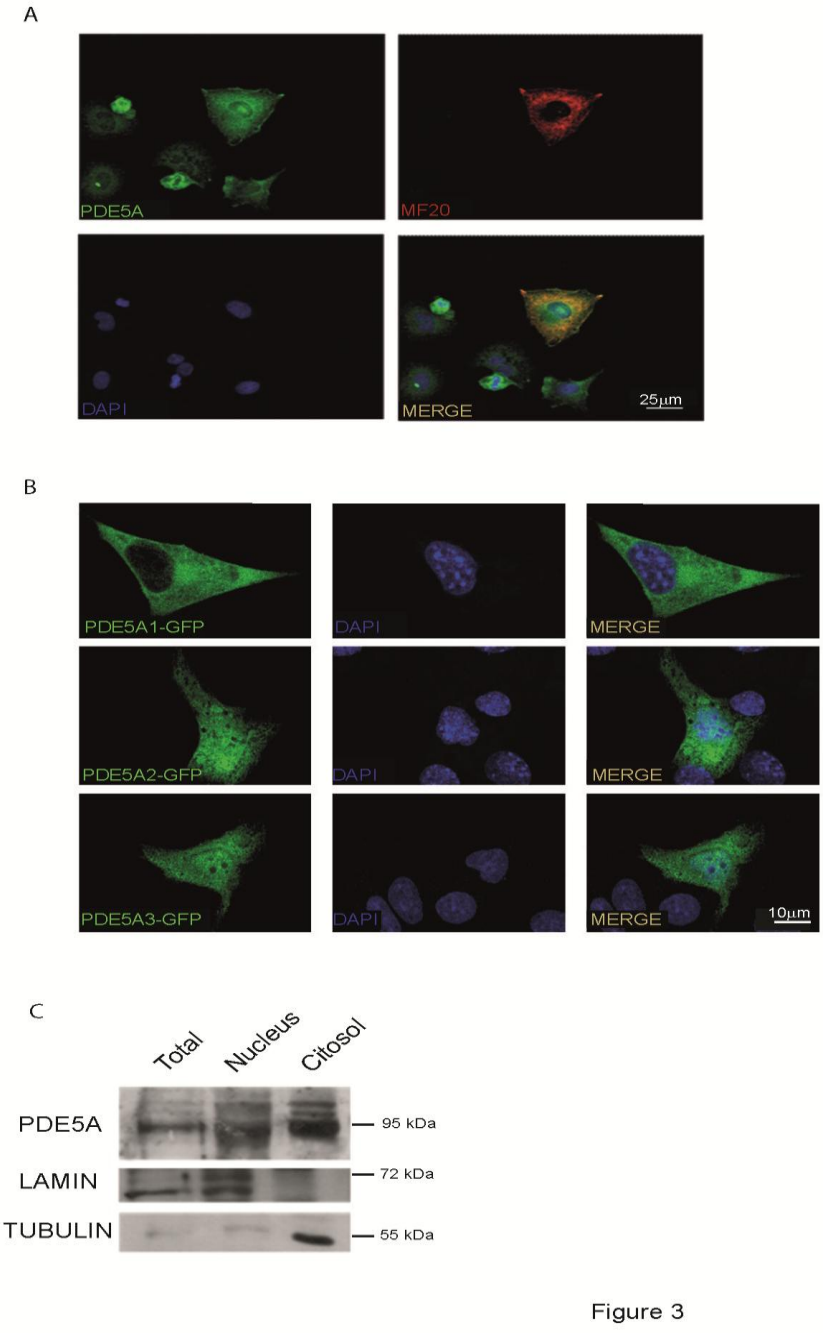

Figure 3

Figure 3

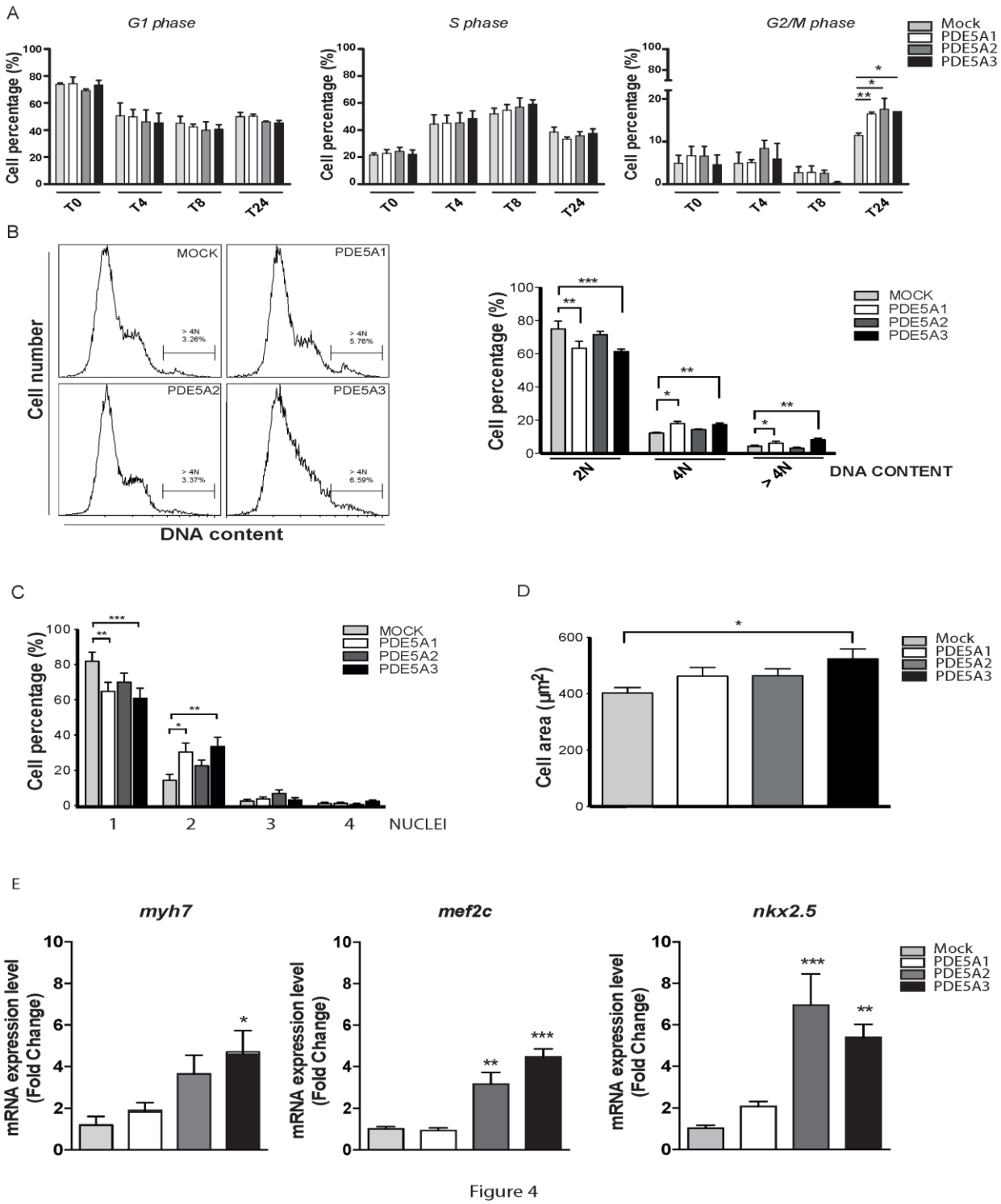

Figure 4

Figure 4